Brazilian Journal of Physics
ISSN: 0103-9733
luizno.bjp@gmail.com
Sociedade Brasileira de Física
Brasil

Elizondo, J.I.; Korneev, D.; Nascimento, I.C.; Sá, W.P. de
TCABR interferometer
Brazilian Journal of Physics, vol. 32, núm. 1, marzo, 2002, pp. 123-130
Sociedade Brasileira de Física
São Paulo, Brasil

TCABR Interferometer

J.I. Elizondo, D. Korneev*, I.C. Nascimento, and W.P. de Sá

Instituto de Física, Universidade de São Paulo,

P.O. Box 66318, 05389-970, São Paulo, Brazil

**ELVA-1 Millimeter Wave Division (DOK Ltd.), St. Petersburg, 193318 Russia*

Received on 26 June, 2001

The microwave interferometer of the TCABR tokamak is presented in this paper, describing in some detail the phase detection procedure and other technical features. The system has three transceivers and seven waveguide channels coupled to horn antennas. The operating frequency, 140 GHz, allows measuring the electronic density of the TCABR plasmas avoiding cutoff and with relatively small refraction effects. The high intermediate frequency, 18 MHz, together with the large pass-band filter and heterodyne detection system allows measuring fast density changes without loss of signal. Some experimental results and calculations are presented.

I Introduction

Microwave interferometry is a well established technique for electronic density measurements in tokamak plasmas (Ref. 1, 2). The principle of operation is based on the phase change that a linear polarized microwave beam, with its electric field parallel to the toroidal field, suffers when it crosses the plasma column. The phase change is proportional to the density integrated along the beam path.

There are several interferometric schemes that allow measuring this phase change during the plasma life time. The microwave interferometer operating in the TCABR tokamak, constructed in St. Petersburg by ELVA, is of the heterodyne type. The basic scheme is shown in Fig. 1. This simplified system will be described first. In the next section some detailed features of the TCABR interferometer will be considered.

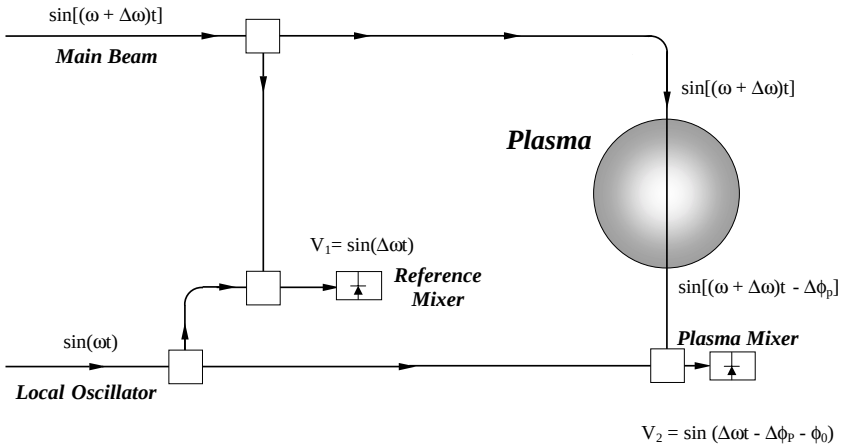

Figure 1. In the heterodyne interferometer, part of the main beam mixes with part of the local oscillator in the reference mixer. After crossing the plasma, the two beams mix again in the plasma mixer. The phase change produced by the plasma is measured from the delay between the two signals.

II Heterodyne interferometer: basic configuration

This type of device has two microwave sources: one for the main beam and the other for the local oscillator. Their frequencies are fixed with values from 60 GHz to 300 GHz, approximately. There is a small difference in frequency, $\Delta\omega$, the intermediate frequency, between the main beam and the local oscillator. In actual interferometers, the intermediate frequency range from 100 KHz to several MHz.

As is well known, when two beams mix in a microwave mixer with Schottky diodes as detectors, the detected signal is sinusoidal, oscillating at the difference frequency of the incoming beam frequencies. So, in the reference mixer (Fig. 1), disregarding amplitude, the signal is

$$V_1(t) = sin(\Delta\omega t). \tag{1}$$

After crossing the plasma column, the main beam suffers a change in phase, $\Delta\phi_p(t)$. This quantity is proportional to the density of the plasma integrated along the beam path (Ref. 1, 3):

$$\Delta\phi_p(t) = 2.82 \cdot 10^{-15}\lambda \int_{z_1}^{z_2} n(z,t)dz, \tag{2}$$

where z_1 and z_2 are the coordinates of the entry and exit points of the beam in the plasma, $n(z,t)$ is the local electronic density and λ is the vacuum wavelength.

The signal at the plasma mixer is

$$V_2(t) = sin(\Delta\omega t - \Delta\phi_p(t) - \phi_0). \tag{3}$$

Without plasma ($\Delta\phi_p = 0$), V_1 and V_2 are sinusoidal signals oscillating at the same frequency, the intermediate frequency, $\Delta\omega$, but they have a fixed phase difference ϕ_0 because of the difference in electrical path between the microwave sources and the mixers (Fig. 2).

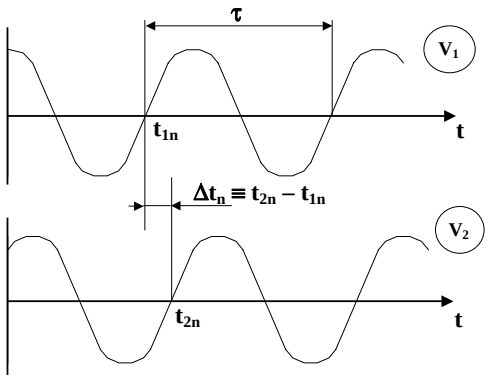

Figure 2. The reference (V_1) and the plasma (V_2) signals. The delay Δt_n between them is a measure of the phase change induced by the plasma, $\Delta\phi_p(t)$.

In the presence of plasma, an additional phase difference $\Delta\phi_p(t)$ is introduced in the V_2 signal producing a delay relative to the reference signal (Fig. 2). This delay vanishes when the plasma shot finishes. Therefore, the plasma density produces a change of phase and this change appears as a delay between two sinusoidal signals.

Many different electronic schemes are used to measure this delay, and, therefore, the change of phase. It will be shown that $\Delta\phi_p(t)$ can be conveniently measured from the zero crossings of the reference and plasma signals, V_1 and V_2. The zero crossings with positive slope, t_{1n} and t_{2n}, correspond to the conditions (Fig. 2):

$$(\Delta\omega)t_{1n} = 2n\pi \rightarrow t_{1n} = \frac{2n\pi}{\Delta\omega} \quad n = 0, 1, 2... \tag{4}$$

$$(\Delta\omega)t_{2n} - \Delta\phi_p - \phi_0 = 2n\pi \rightarrow t_{2n} = \frac{2n\pi + \Delta\phi_p + \phi_0}{\Delta\omega} \tag{5}$$

$$\Delta t_n \equiv t_{2n} - t_{1n} = \frac{\Delta\phi_p(t) + \phi_0}{\Delta\omega} \tag{6}$$

Equation (6) is very important since it relates the time interval between zero crossings to the phase change.

The value of $\Delta\omega$ is obtained directly from V_1. It is easy to determine ϕ_0 by measuring Δt_n before the breakdown of the gas ($\Delta\phi_p = 0$). In this way, $\Delta\phi_p(t)$ is univocally determined by Δt_n measurements, using (6).

Calculating density from time measurements (see Eq. 6) instead of amplitude signal measurements, as in older interferometers, presents two main advantages:

- Amplitude changes produced by refraction, absorption, etc., do not influence the results.
- The scheme avoids ambiguity of interpretation at the maxima and minima signal points (Ref. 3). As can be seen from (6), the signal of phase variation (and therefore density variation) at each time is provided unambiguously by time measurements.

III Description of the TCABR interferometer

The principle of operation of this interferometer is basically the same of the simplified interferometer described in the previous section.

The interferometer has three transceivers operating at slightly different frequencies (Table 1). The transceivers can be connected to seven oversized waveguides ended by horn antennas. The radial positions of the channels relative to the plasma center are shown in Table 2.

Table 1 - Transmitter and Local Oscillator frequencies for the three microwave channels.

	Frequency (GHz)	
Channel No.	Transmitter	Local Oscillator
1	140.842	140.860
2	140.000	140.018
3	139.000	139.018

Table 2 - Radial position $(R - R_0)$ of the seven vertical chords relative to the plasma center.

Chord No.	$(\boldsymbol{R}$-$\boldsymbol{R}_0)$ [cm]
-3	-17
-2	-12
-1	-6
0	-1
1	4
2	9
3	14

The block diagram of one transceiver is displayed in Fig. 3 and the following discussions refer to this figure.

The transmitter has a gallium arsenide transistor in a DRO (Dielectric Resonant Oscillator). This device oscillates with very high frequency stability ($\Delta f/f \leq 5.10^{-6}$). The output is coupled to a power amplifier of 800 mW output power that drive an IMPATT diode. This non-linear device generates harmonics of the fundamental frequency. A waveguide pass-band filter selects the 18^{th} harmonic, at approximately 140 GHz.

The local oscillator is analogous to the transmitter, yet there is a small difference between the frequencies of the DROs. This difference, multiplied by 18 in the IMPATT diode, is the intermediate frequency (IF), named $\Delta\omega$ in the previous section.

Before the frequency is multiplied, a small fraction of the microwave power of the LO (local oscillator) and the TR (transmitter) is mixed in the reference mixer. The obtained 1 MHz sinusoidal signal is the reference signal of the interferometer. In spite of the great frequency stability of the DROs, this frequency may shift from 1 MHz, but if the drift is not too large the interferometer will operate satisfactorily.

The main microwave beam, from the transmitter, crosses the plasma column, changing its phase by an amount $\Delta\phi_p(t)$. After mixing with the LO beam in the balanced mixer, the output signal is sinusoidal, as described by (3), but the amplitude is not constant due to beam refraction and absorption in the plasma (Fig. 4, plot 1).

The passive filter, centered at 18 MHz, has ± 2 MHz passband width. The choice of this pass-band is a compromise between noise rejection (narrow band) and speed (wide band). Speed, in this context, is the interferometer ability in following quick changes in density without loss of signal.

The amplifier, with output limiter, converts the sinusoidal signal in an approximately square wave train, as can be seen in Fig. 4, plot 2. The frequency of this signal is electronically divided by 18, and so the output signal is a 1 MHz square wave (Fig. 4, plot 3). In the following this signal will be named the plasma signal.

Also the reference signal from the reference mixer is converted in a square wave of the same frequency, 1 MHz (Fig. 4, plot 5). The phase change induced by the plasma produces a delay between both square waves. These two signals are connected to the SPU (Signal Processing Unit), twenty meters away from the interferometer, using twisted pair cables.

Several methods are available for determining the delay between the two square waves. The method applied in this SPU will be described in the following (Figs. 5 and 6).

The rising edge of one clock signal triggers a ramp voltage and the falling edge of the following fourth pulse determines the falling of the ramp. In this manner is produced a 250 KHz sawtooth voltage (Fig. 5, plot 7). The sawtooth is connected to the ADC module (Fig. 6). The acquisition rate of the ADC is controlled by the falling edge of the square wave from the plasma mixer. During the sawtooth falling is generated a blocking pulse, avoiding the ADC reading any signal (Fig. 5, plots 6 and 7).

In this way, the data stored in the ADC are a set of voltage values. It is easy to see from Fig. 5 that any shift in the plasma signal relative to the sawtooth produces a change in the acquired data: the amplitudes encode the phase change produced by the plasma.

If plotted, the stored data without plasma appear as three horizontal lines. When plasma is created, there is a change in phase, therefore the square train of the plasma signal shifts to the right relative to the sawtooth (Fig. 5) and the stored values increase. When density decreases also the stored values decrease.

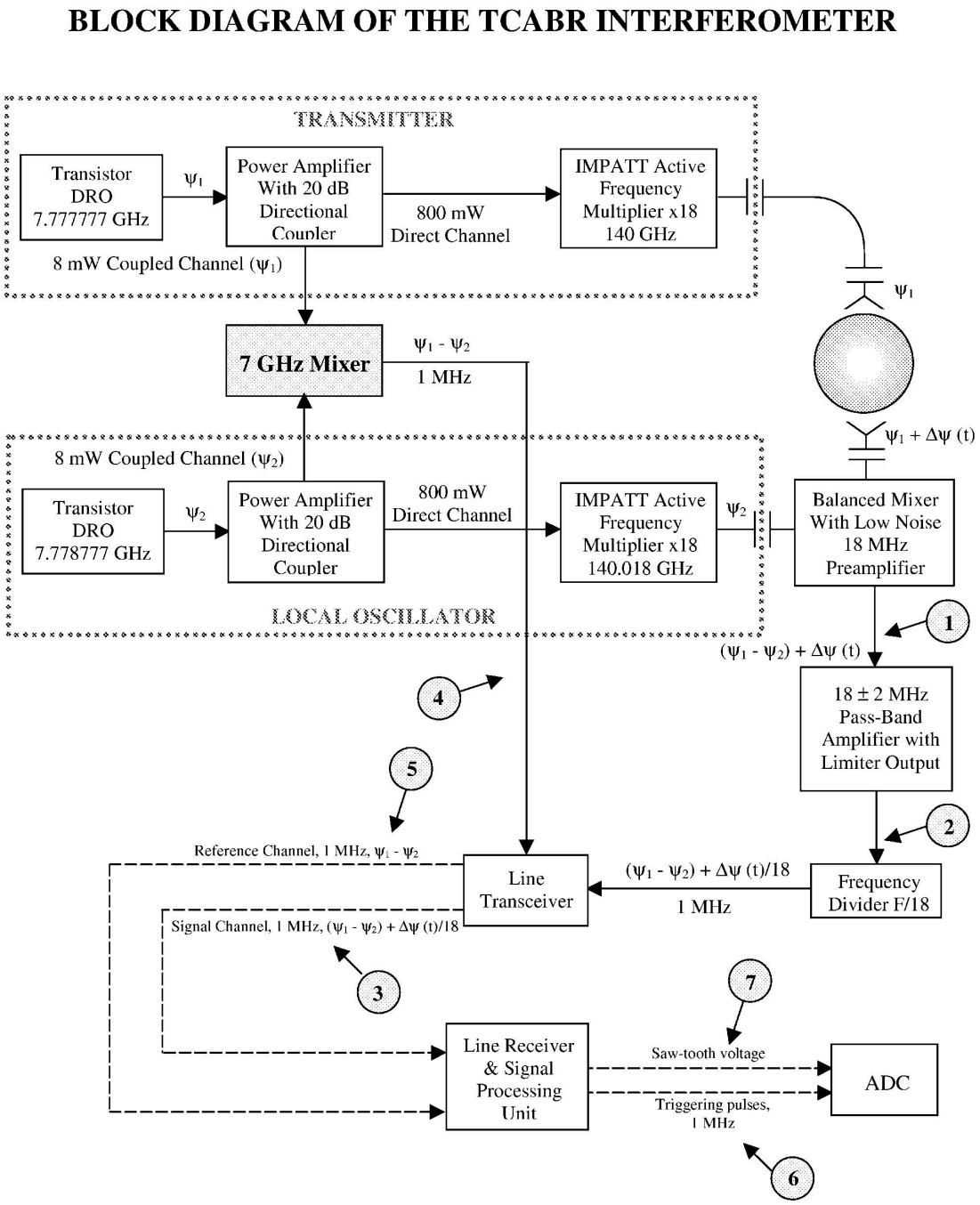

Figure 3. The block diagram of the TCABR interferometer has the same basic configuration of the simple heterodyne interferometer shown in Fig. 1. The encircled numbers refer to the same numbers in Figs. 4 and 5.

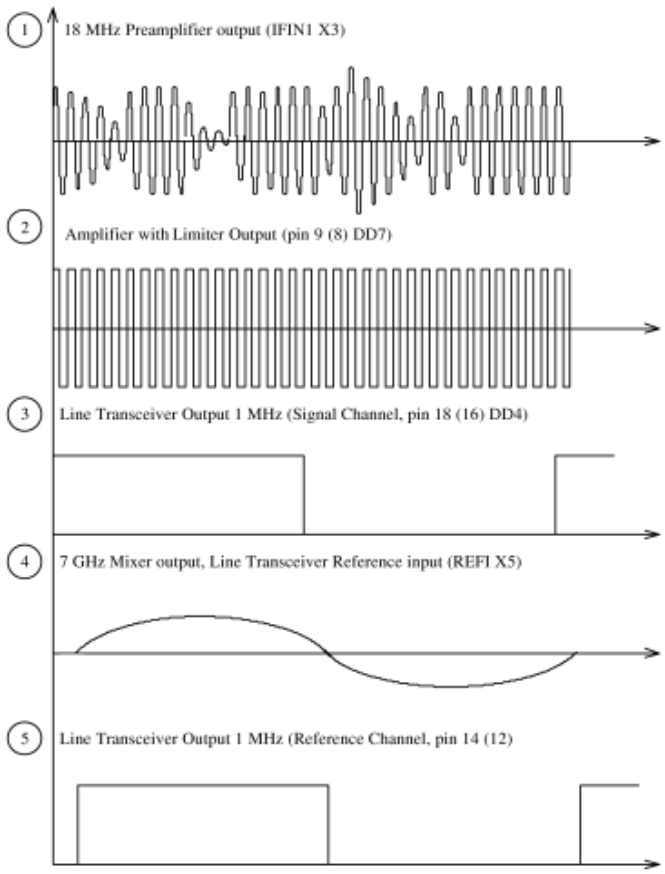

Figure 4. Main signals in the transceiver of the TCABR interferometer. The encircled numbers refer to the same numbers in Fig. 3.

IV Calculation of the line density from the data

The line density, $\bar{n}$, is defined as

$$\bar{n}(t) \equiv \frac{1}{(z_2 - z_1)} \int_{z_1}^{z_2} n(z,t) dz \tag{7}$$

and using (2):

$$\bar{n}(t) = \frac{1}{(z_2 - z_1)} \frac{\Delta\Phi_p(t)}{2.82 \cdot 10^{-15}\lambda)} \tag{8}$$

For a vertical beam crossing the plasma center, (8) can be written

$$\bar{n}(t) = 4.6 \cdot 10^{17} \Delta\phi_p(t). \tag{9}$$

Without plasma, the stored points are sequences of three increasing values. Each sequence, disregarding noise, has the same values as the others. If V_j^0 and V_{j+1}^0 are two neighbor points with $V_{j+1}^0 > V_j^0$, the difference $\Delta V_{j+1}^1 \equiv V_{j+1}^0 - V_j^0$ corresponds to a period of the plasma square wave, τ, and, therefore, a change in phase of 2π. But, as the frequency of the plasma signal was divided by 18, ΔV_1^0 corresponds to a 36π change in the intermediate frequency, $\Delta\omega$:

$$36\pi = k \cdot \Delta V_1^0 \tag{10}$$

where k, the scale factor, relates the change in the signal amplitude with the change in phase, and therefore, with the change in density. This procedure does not use (6) explicitly, but is equivalent to it.

In every plasma shot, the ADC stores data from several milliseconds before the breakdown. The computer program that calculates the density uses these data without plasma to determine k from (10). All data corresponding to a shot are separated in three vectors, V^1, V^2 and V^3, where V^1 corresponds to points with index 1, 4, 7..., V^2 contains points with indexes 2, 5, 8... and so on.

The time evolution of the density is calculated independently from the three vectors. This redundancy may be used to eliminate errors. The change in phase corresponding to the values V_j^1 and V_{j+1}^1 is easily calculated:

$$\Delta\phi_{j+1,j}^1 = k(V_{j+1}^1 - V_j^1). \tag{11}$$

The density change can be calculated by substituting (11) into (8) and the time dependence of the density during the discharge is obtained by adding the density changes.

Untill now nothing has been said about the time scale. The time interval between ADC stored points corresponds to the period of the plasma signal without plasma disregarding the small variations in time induced for $\Delta\phi_p(t)$, as can be seen by (3). The frequency of the plasma signal is approximately 1 MHz, but this frequency may drift because it depends on the frequency difference of transmitter and local oscillator DROs. Thermal variations, for instance, can produce small changes in DRO frequencies. So it is convenient to measure the frequency of the plasma signal in each shot. This is accomplished connecting a crystal, whose period is 1 ms, to one channel of the ADC; the acquisition rate is controlled by the plasma signal (Fig. 6). The crystal output, operating in monostable mode, is triggered 5 ms before the breakdown. When the signal is high, the number N of high level points recorded in the ADC is determined by the relation

$$\left(\frac{4}{3}N - 0.5\right) \cdot \tau = 1 \cdot 10^{-3} \qquad (12)$$

where τ is the period of the plasma signal. The 4/3 factor compensates for the forbidden pulse in the falling edge of the sawtooth (Fig. 5, plot 7). The program that calculates the density also determines the time scale τ using (12).

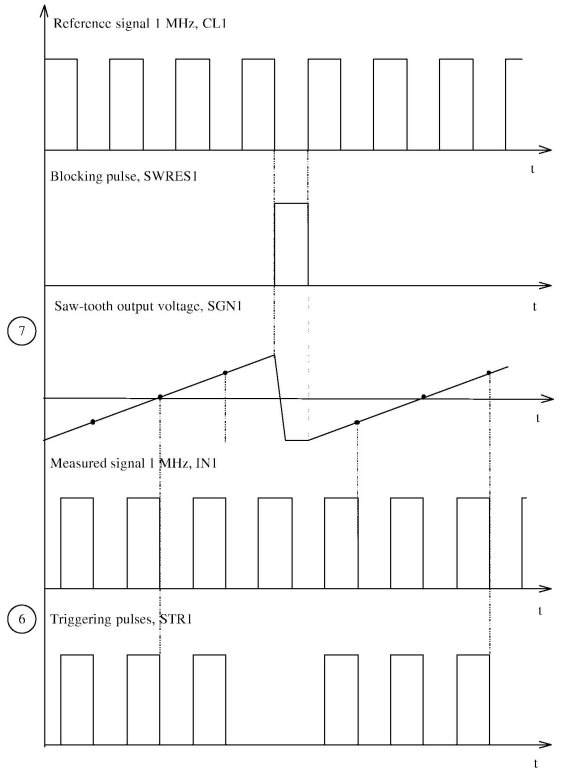

Figure 5. Main signals in the Signal Processing Unit (SPU) of the TCABR interferometer. The encircled numbers refer to the same numbers in Fig. 3.

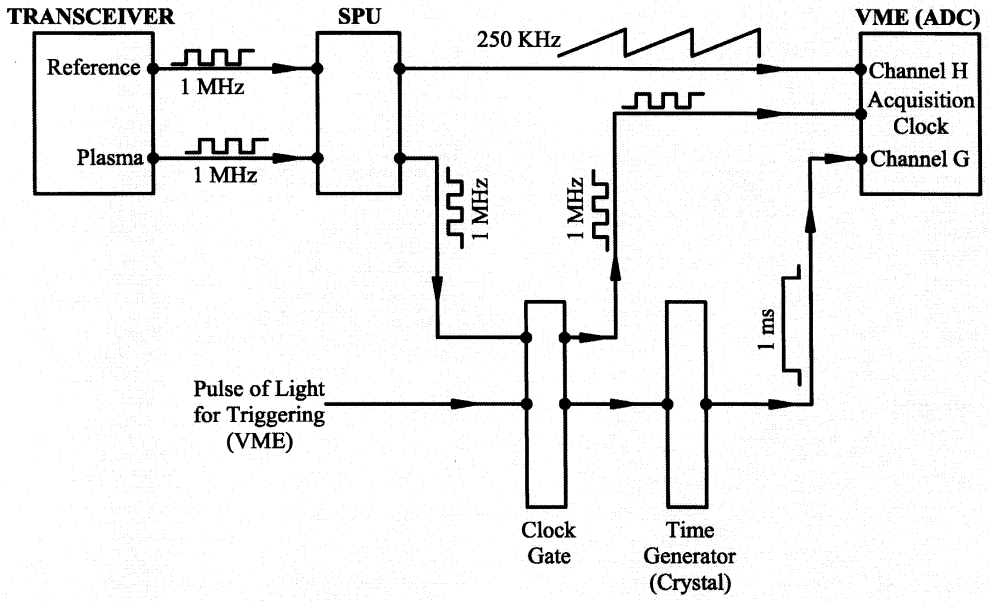

Figure 6. Block diagram of the connection between the transceiver of the interferometer and the ADC (VME). The triggering is performed 5 ms before the breakdown, allowing the ADC module to store data before and during the plasma shot.

V Performance calculation

Speed

The maximum speed of the interferometer corresponds to the maximum rate of change in density that the interferometer can follow without loosing of signal.

If the change in density is so fast that the total rate of phase change exceeds (disregarding the factor 2π) 18 ± 2 MHz, the signal will be out of the filter band and will not be detected. From (3), the change in phase from t_1 to t_2 is:

$$\Delta\varphi = [\Delta\omega(t_2 - t_1) - (\Delta\phi_p(t_2) - \Delta\phi_p(t_1))] \ . \quad (13)$$

Defining M as the maximum allowable rate of total phase change,

$$M \equiv \frac{1}{2\pi}\frac{\Delta\varphi}{(t_2 - t_1)}\Big|_{\max} = \frac{1}{2\pi}\left[\Delta\omega - \frac{(\Delta\phi_p(t_2) - \Delta\phi_p(t_1))}{(t_2 - t_1)}\right|_{\max}, \quad (14)$$

it is clear that $M = 18 \pm 2$ MHz and the maximum allowable rate change of phase induced by the plasma is

$$\left|\frac{(\Delta\phi_p(t_2) - \Delta\phi_p(t_1))}{(t_2 - t_1)}\right| \leq 2\pi(2 \cdot 10^6) rad.s^{-1} \quad (15)$$

This value corresponds to a density change rate of $5.8 \cdot 10^{24}\mathrm{m}^{-3}\mathrm{s}^{-1}$, as can be seen from (9).

b. Sensitivity

The interferometer sensitivity is the minimum detectable density change. This corresponds to a change of one level in the ADC. The ADC of the interferometer has 12 bits (4,096 levels) and the maximum input of every channel is $\pm$ 2.5 V. For a sawtooth voltage of 4 V (peak to peak) every level corresponds, therefore, to 1 mV, approximately.

The scale factor, k, calculated by (10), depends on the actual amplitude of the sawtooth. For 4 V, the difference between neighbor values is $\Delta V_1^0 = 1V$ and $k = 36\pi$ rad.V^{-1}. For this case, the phase change corresponding to 1 mV, calculated by (11), is 11°, and the corresponding line density, using (9), is $5.2 \cdot 10^{16}$ m^{-3}.

c. Refraction and critical density

The microwave wavelength inside the plasma increases with density. When density approaches the critical density, the wavelength diverges and the beam is reflected. The critical density, n_c, corresponds to the value for which the plasma frequency equals the microwave frequency:

$$n_c = \frac{4\pi^2 c^2}{\lambda^2}\frac{\epsilon_0 m_e}{e^2} = \frac{1.1 \cdot 10^{15}}{\lambda^2} \ , \quad (16)$$

where λ is the vacuum wavelength and ε_0 is the vacuum permitivity.

For the 140 GHz interferometer ($\lambda = 2.1$ mm), n_c is $2.4 \cdot 10^{20}$ m^{-3}, four times greater than the maximum density measured in the TCABR tokamak. So, no problems related with critical density are expected.

Refraction depends on the gradients of density perpendicular to the line propagation of the beam. For a parabolic density profile, the angle α between the direction of propagation of the incoming and the exiting beams can be analytically calculated (Ref. 4). The maximum refraction angle, α_m, corresponds to $r \approx 0.7a$, where a is the plasma radius and r is the radial coordinate (Ref. 3):

$$\alpha_m = sin^{-1}\frac{n_0}{n_c} \cong \frac{n_0}{n_c} = \frac{e^2}{4\pi^2 c^2 \epsilon_0 m_e} n_0\lambda^2 = 8.97 \cdot 10^{-16} n_0\lambda^2, \quad (17)$$

where n_0 is the density in the center of the column.

For $n_0 = 5 \cdot 10^{19}$ m^{-3}, using (17), the calculated maximum refraction angle is $\alpha_m \cong 0.2rd \cong 12°$. This value is relatively small, and the decreasing of the detected signal during the shot related with refraction will be not very high.

VI Experimental results

The interferometer was used for density measurements in excess of four thousands plasma shots. The noise level, without plasma, is equivalent to densities between $(0.5 - 2) \cdot 10^{18}$ m^{-3}, limiting the real sensitivity of the interferometer, but this value can be optimized carefully adjusting the electronics of the receiving system and the SPU.

Fig. 7 shows the results obtained in a TCABR shot for two different channels (distinct radial positions). Enlarging any portion of the flat top it is possible to

see clearly a periodical fluctuation whose frequency is approximately 11 kHz. This frequency agrees very well with the MHD frequency measured at the same time by special coils located inside the vacuum vessel. It will be necessary to study with more detail the connection between MHD oscillations and density oscillations.

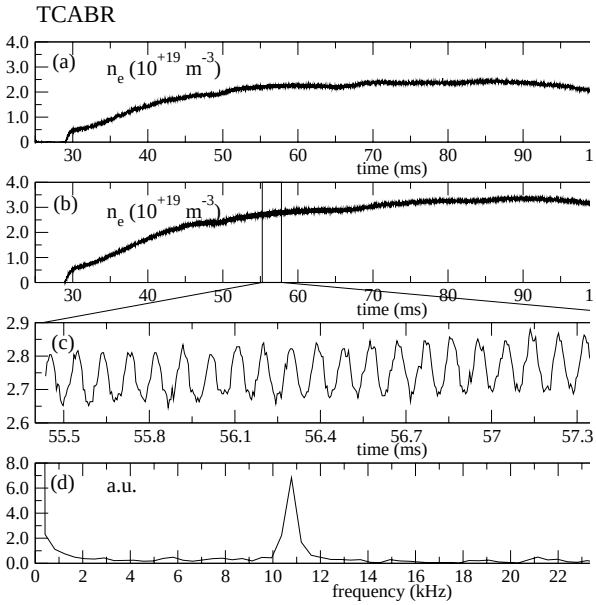

Figure 7. (a) Time history of plasma density calculated from the data obtained by the interferometer in the plasma shot # 3029. (a) Plasma vertical chord with $R - R_0 = -1$ cm; (b) Plasma vertical chord with $R - R_0 = 4$ cm; (c) Expanded plot of part of the density curve; (d) Fast Fourier Transform of the data shown in plot (c). The frequency of the signal is approximately 11 kHz, as the MHD signal detected by pick up coils.

Acknowledgements

We would like to thank A. Sergeev and the ELVA team for the fruitful discussions, A. P. dos Reis for developing and testing electronic circuits associated with the interferometer and A. Candido for some of the drawings in this paper and FAPESP and FINEP for the financial support of this work.

References

[1] M.A. Heald and C.B. Wharton, *Plasma Diagnostics with Microwaves*, John Wiley & Sons Inc., New York, 1965.

[2] A.J.H. Donné, "High spatial resolution interferometry and polarimetry in hot plasmas", Rev. Sci. Instrum. **66**, 3407 (1995).

[3] D. Véron, *Submillimeter Interferometry of High-Density Plasmas* in Button, K.J. (Editor) "Infrared and Millimeter Waves", Vol. 2, Academic Press, New York, 1979.

[4] J. Shmoys, "Proposed Diagnostic Method for Cylindrical Plasmas", Journal of Applied Physics, **32,** 689 (1961)